Investigation of Bonnet Leading Edge Stiffness for the Reduction of Leg, Pelvis and Head Injuries during SUV-Pedestrian Impact

Daniel Isemann, Alexander Besch, Karina Lehmann, Martin Böhme, Matthias Kröger

Abstract The advanced Pedestrian Legform Impactor (aPLI) was introduced for the assessment of pedestrian safety, which considers femur injury criteria and represents, in particular, SUV-pedestrian accidents more realistically compared to its predecessor the Flexible Pedestrian Legform Impactor (FlexPLI). However, designing pedestrian friendly SUV front-ends not only involves reducing lower extremity injuries but also pelvis and head injuries. In this study, we investigate the bonnet leading edge (BLE), which is a critical area for all three types of injuries, using a detailed Finite Element Method (FEM) SUV model with sensitivity analyses at the two test positions *Y0* and *Y+600* (at the vehicle centre and at the right headlight from driver's perspective). Thereby, we decompose the BLE into its horizontal and vertical stiffness components and show that a horizontally weaker BLE helps to decrease all relevant injury values for both test positions. Further, we show that a vertically stiffer BLE helps to reduce the leg and pelvis injury values at test position Y+600 even for a wide range of shooting heights. However, this subsequently increases the head injury criterion (HIC) value significantly, which gives rise of motivation to actively control the BLE's vertical stiffness depending on the individual load case (weak vertical stiffness for head impact and stiffer vertical stiffness for leg/pelvis impact).

Keywords aPLI, bonnet leading edge, HIC, pedestrian safety, pelvis injuries.

I. INTRODUCTION

In 2016, the World Health Organization reported 1.35 million road traffic fatalities worldwide. Vulnerable Road Users (VRUs) account for 54% of the reported fatalities: motorcyclists (28%), pedestrians (23%) and cyclists (3%) [1]. In 2021, pedestrian fatalities account for 17% of all road fatalities in the United States of America (US) and for 20% of all road fatalities in the European Union (EU). In urban areas, however, this rises to 32% in the US and to 38% in the EU [2].

In 2019, 17.7 million incidences of injured pedestrians were estimated globally [3]. By analysing the German In-Depth Accident Study (GIDAS), [4] found that lower limb injuries are, by far, the most frequently injured body region of any injured pedestrians in Germany (67%). Additionally, the Disability-Adjusted Life Year[1] for the 10 leading global burden of diseases ranks pedestrian injuries at 9th in 1990 and at 3rd in 2020 [3], [5]. Overall, lower extremity injuries account for 33% of pedestrian Abbreviated Injury Scale (AIS) 2+ injuries in vehicle-to-pedestrian collisions [6-7]. To counteract these developments, the *Euro NCAP* VRU assessment protocol (v11.2.2) introduces the advanced Pedestrian Legform Impactor (aPLI) and replaces the Flexible Pedestrian Legform Impactor (FlexPLI) to assess vehicle safety during vehicle-pedestrian leg impacts. The aPLI has additional femur bending moment measuring sensors to evaluate the leg impact more comprehensively. On the other hand, vehicles tend to increase in size and weight. Within a decade, the share of SUVs in new sales for the European market had risen from 8.5% in 2009 to approx. 40% in 2020 [8]. In the US, this share has risen from 27% to approx. 50% [9].

Vehicle front-end design parameters influence the risk of injury in a pedestrian collision [10-11]. This study

[1]A health-gap measure that combines information on the number of years lost from premature death with the loss of health from disability.

D. Isemann (e-mail: daniel.isemann@volkswagen.de; tel: +49 1525 4914881) is a doctoral student at Volkswagen AG and at TU Bergakademie Freiberg, Germany. Dr. rer. nat. A. Besch and Dr.-Ing. M. Böhme are Engineers at Volkswagen AG in Wolfsburg, Germany. K. Lehmann is an Engineer at VAIVA GmbH in Gaimersheim, Germany. Prof. Dr.-Ing. M. Kröger is a Professor and Chairman at the Institute of Machine Elements, Design and Manufacturing (IMKF) at TU Bergakademie Freiberg, Germany.

analyses the bonnet leading edge (BLE) in SUV-to-pedestrian collisions, which affects leg, pelvis and head impact load cases. The objective is to identify design parameters for a balanced consideration of all three types of pedestrian injuries. Nevertheless, optimising the front-end for a specific injury criterion (i.e. reduction of femur bending moment) in vehicle-to-pedestrian collisions can simultaneously increase other injury criteria (i.e. increase of tibia bending moment) [12-13]. Consequently, this study considers all three types of injuries (leg, pelvis and head), focusing on the newly added aPLI femur criteria.

Overall, there is a critical need for research regarding lower extremity injuries in SUV-to-pedestrian collisions. This paper contributes to this in two ways. First, an in-depth analysis investigates horizontal and vertical stiffness of the BLE with respect to the aPLI injury criteria, the human body model (HBM) pelvis contact forces and the head injury criterion (HIC) measured with the child headform impactor. Second, a variation of the aPLI's and HBM's shooting height is conducted to establish a valid range for the most optimal BLE, based on the results of the horizontal and vertical stiffness decomposition.

II. METHODS

In this study, sensitivity analyses are conducted exclusively using finite element method (FEM) simulations. All simulations are performed using the dynamic explicit solver Virtual Performance Solution of the ESI group. A single, state of the art, SUV front-end model is examined, which consists of more than three million elements. The aPLI, the THUMS AM50 v4.02 pedestrian model and the child pedestrian headform impactor are the subjects of this study. To investigate the BLE stiffness on the aPLI injury criteria (focusing on the femur bending moments) and the pelvis of the HBM, the simulations are conducted at the outermost test position of the Euro NCAP grid on the passenger's side (right side from driver's perspective at Y+600) and at the central test position (Y0) for the HBM and the aPLI. The headform impactor test positions correspond to Y0 and Y+600, impacting the BLE area in the foremost Euro NCAP test position. The design parameters are investigated with a Design of Experiments of 100 points for the aPLI, HBM and child headform impactor. The points are sampled according to an optimised Latin Hypercube. Linear regression is performed to determine the Pearson correlation coefficient r and the slope α of the regression lines between the design parameters and the injury values. The injury values and the design parameters are expressed in relation to the original vehicle (i.e. 1.5 times the Bonnet's exterior sheet thickness corresponds to 3 mm for an original bonnet's exterior sheet thickness of 2 mm; 1.5 times the femur bending moment corresponds to 300 Nm for an original femur bending moment of 200 Nm).

For all simulations with the aPLI, HBM and child headform impactor, the impact velocity is 40 kph. The interval of evaluation for the injury criteria is set to 60 ms, starting from the initial impactor-vehicle (or vehicle-HBM) contact. For each HBM simulation the left leg is initially impacted and evaluated.

Positioning of the human body model

In [14] it was shown that the aPLI produces symmetrical injury values regardless of whether the right or the left headlight area of a vehicle is impacted. However, the posture of the HBM and especially its non-struck leg positioning can significantly affect the resulting injury values in oblique impact positions, which may limit its acceptability for comparison with the aPLI. Therefore, two characteristic HBM postures with the vehicle models in [14] are compared in terms of their maximum *MCL* elongation values. The first investigated posture of the HBM (straight left leg carrying the entire weight and right leg inclined 20° forward) shows maximum non-struck leg influence and is commonly used [15-18]. The second posture has minimum non-struck leg influence due to neutral non-struck leg positioning (20% gait position in [19]) and is part of a realistic gait cycle.

Decomposition of bonnet leading edge stiffness into its horizontal and vertical components

The BLE consists of the bonnet's exterior sheet, the bonnet's interior sheet and a support part. Figure 1 shows the aPLI impact kinematics for the basic SUV configuration to analyse, which of the parts predominantly define vertical or horizontal stiffness. Based on this, the design parameters for the sensitivity analyses are derived.

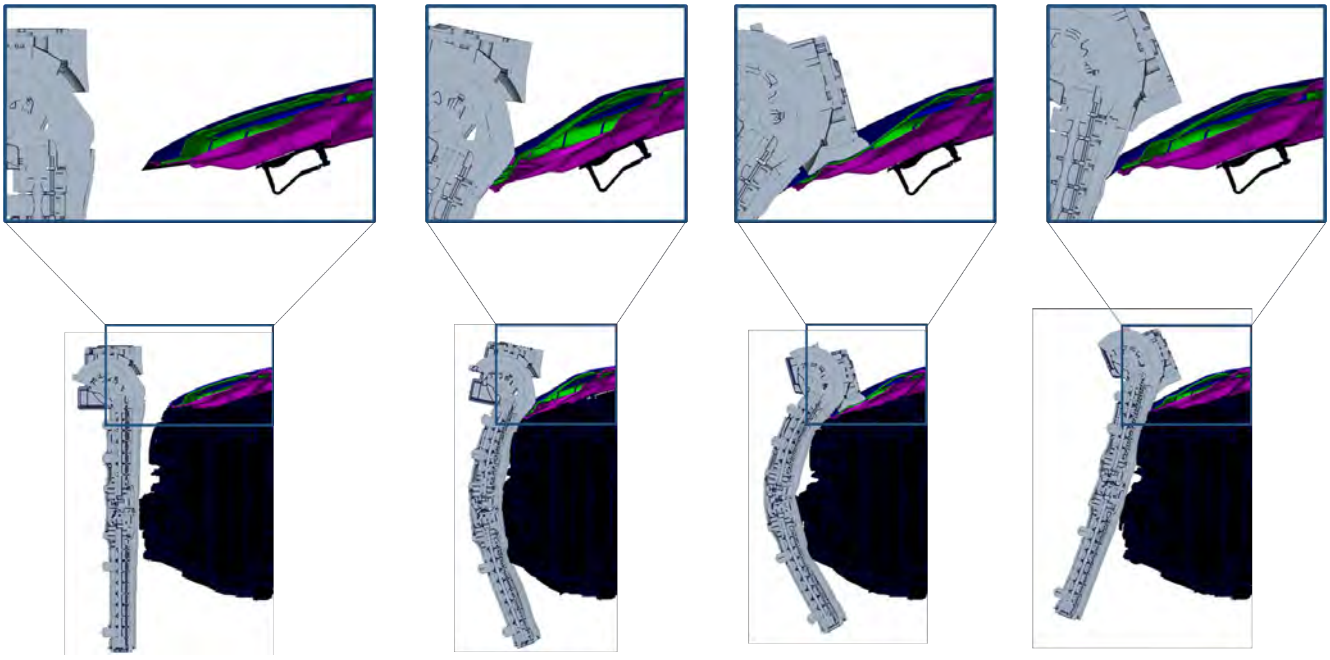

(a) t = 0 ms (b) t = 20 ms (c) t = 40 ms (d) t = 60 ms

Fig. 1. APLI impact kinematics at test position Y0 of the SUV in full section (lower row) focusing on the deformation behavior of the bonnet's exterior sheet (blue), the support part (green) and the interior sheet (magenta) (upper row).

Figure 1 shows that the bonnet is impacted by the simplified upper body part (SUBP) of the aPLI. The interior sheet (magenta) and the front of the support part (green) influence the horizontal stiffness whereas the exterior sheet (blue) influences mainly the vertical stiffness. Overall, the BLE package for this SUV is stiff in the horizontal direction and deformable in the vertical direction.

Therefore, the variation of the bonnet's exterior sheet thickness is the parameter of choice for the investigation of vertical stiffness in the BLE area. However, in order to investigate the horizontal stiffness, both the support part and the interior plate (as a bearing for the support part) would also influence the vertical stiffness. For this reason, ribs are used in the foremost area between the exterior and the interior sheet at a constant distance of 10 cm across the vehicle width, which is shown in Figure 2. The rib thickness is the parameter of choice for investigating an increased horizontal stiffness.

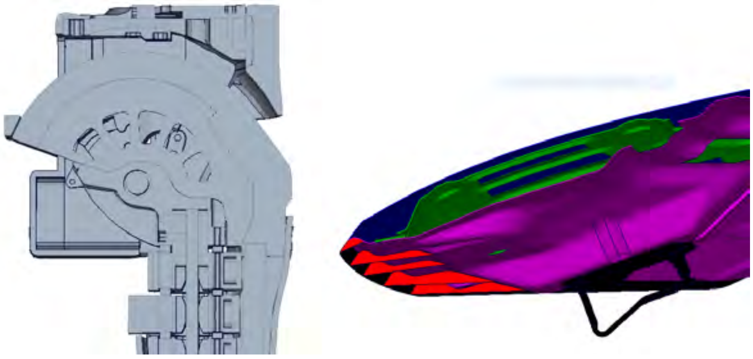

Fig. 2. Implementation of ribs (red) between the exterior and interior sheet (full section at Y0).

To investigate a reduced horizontal stiffness, while maintaining realism, the front area of the support part, which was in parallel alignment to the interior sheet, is modified. Figure 3 illustrates the modification.

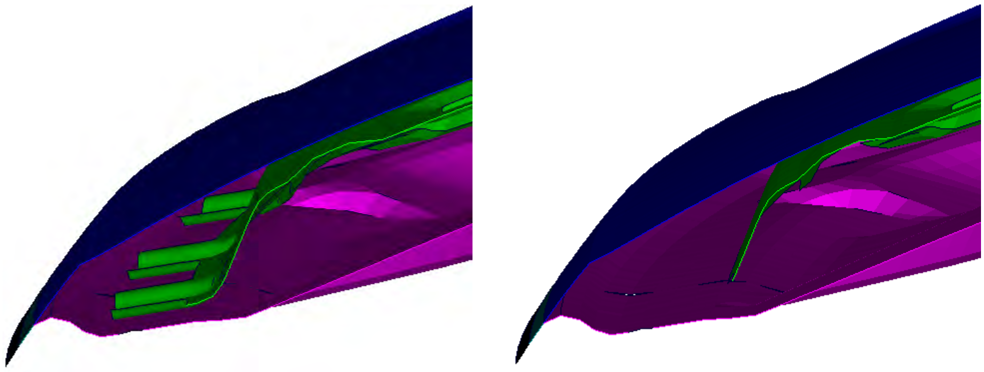

(a) Original (b) Modified

Fig. 3. Comparison of the original support part (a) and the modified support part (b) between the exterior and interior sheet (full section at Y0).

In order to analyse the horizontally weaker BLE, the injury values based on the modified support part are directly compared with the original values. It should be noted that linear regression is not employed in this instance, as the modification is not performed iteratively but only consists of a single simulation.

Finally, based on the results of the ideal horizontal BLE stiffness, contour plots are employed to investigate the combined variation of vertical stiffness (variation of exterior sheet thickness by ±50%) and shooting height on the aPLI and HBM injury criteria. This investigation tries to account for varying pedestrian heights.

III. RESULTS

Positioning of the Human Body Model

Figure 4 shows the comparison of the MCL elongation values for the HBM in the posture analogous to [15-18] (straight left leg carrying the entire weight and right leg inclined 20° forward) and the posture with a more neutral non-struck leg position (20% gait position in [19]) with the vehicle models used in [14].

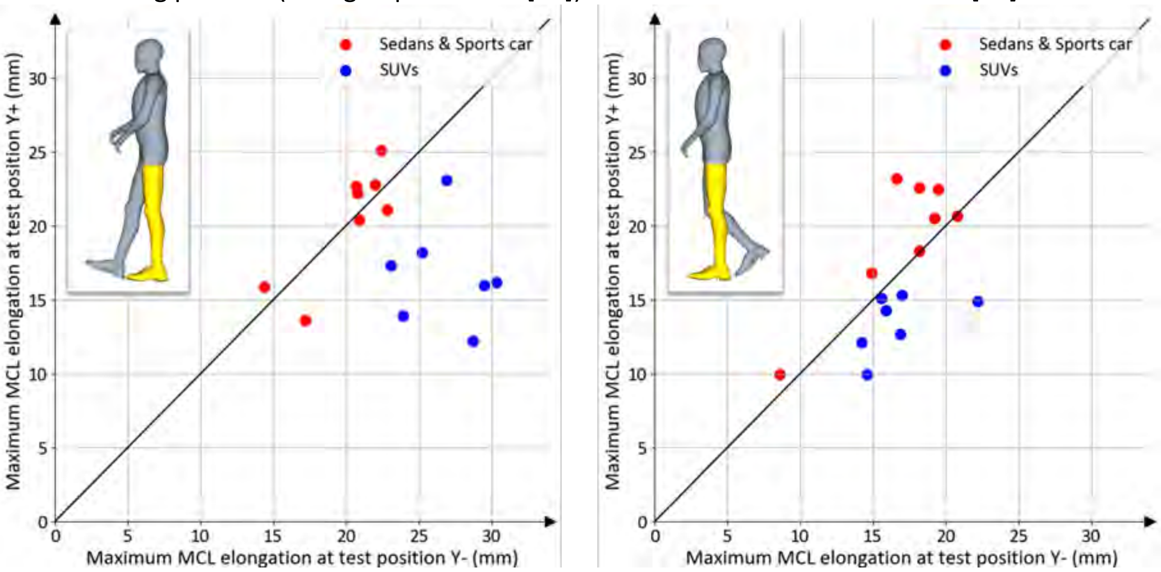

(a) (b)

Fig. 4. Results of the maximum MCL elongation values obtained from real car model FEM simulations for the outermost Euro NCAP test positions Y- and Y+ (Y+ on the right and Y- on the left from the driver's perspective) using the HBM in a posture with (a) the non-struck leg inclined 20° forward and (b) the non-struck leg in a more neutral position.

Figure 4 indicates that the HBM posture with the neutral non-struck leg (Figure 4b) leads to significantly more symmetrical injury values compared to the posture with the 20° forward inclined non-struck leg (Figure 4a). Therefore, the following investigations in this paper are conducted with the posture in Figure 4b, which is also part of a realistic gait cycle.

Variation of Vertical Stiffness at Test Position Y0

The aPLI, HBM and child headform impactor results for the variation of vertical BLE stiffness (variation of the bonnet's exterior sheet thickness) against the SUV at test position Y0 are shown in Figure 5 and Figure 6. Figure 5 contains the results for the leg and head measurements and Figure 6 contains the HBM pelvis measurements.

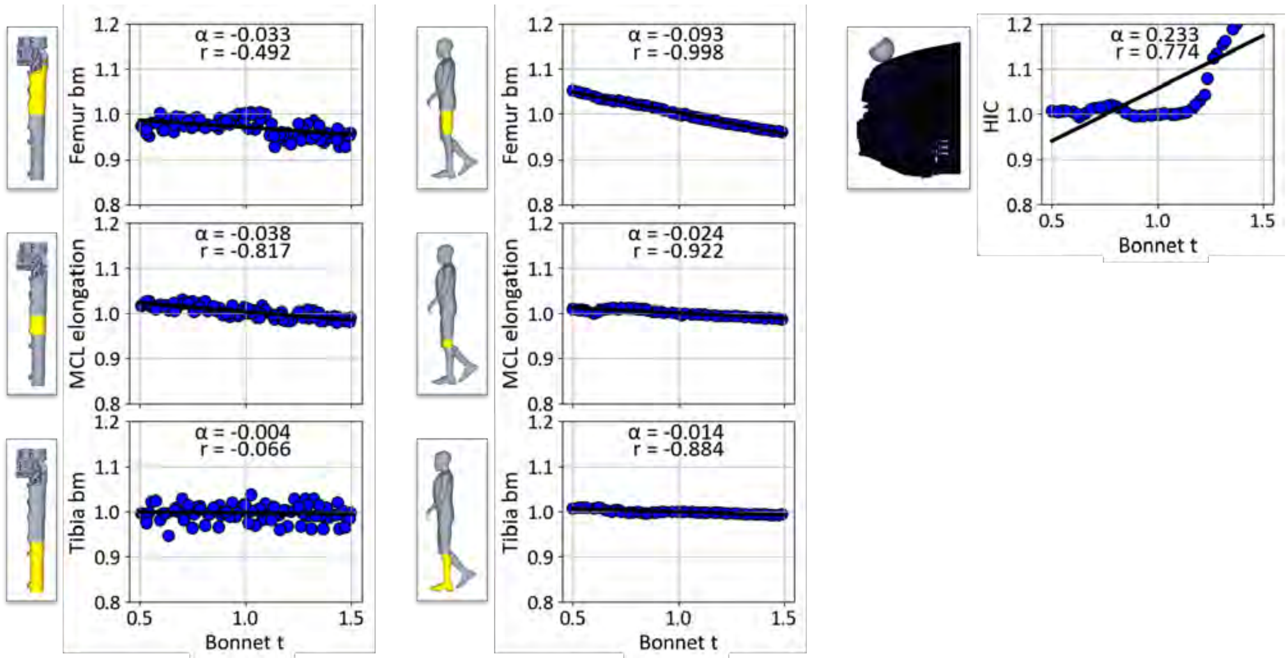

(a) aPLI (b) HBM (c) Child headform impactor

Fig. 5. Normalised maximum injury values for (a) the aPLI, (b) the HBM leg and (c) the child headform impactor (HIC) at test position Y0 for the SUV by varying the exterior sheet thickness of the bonnet.

A stiffer bonnet in the vertical direction (increase of the bonnet's exterior sheet thickness) shows reduced injury values for the aPLI and the HBM's struck leg holistically. Especially the maximum HBM femur bending moment gets decreased significantly. However, the HIC values increase drastically once the bonnet's exterior sheet thickness (Bonnet t) exceeds 1.2 times its original value.

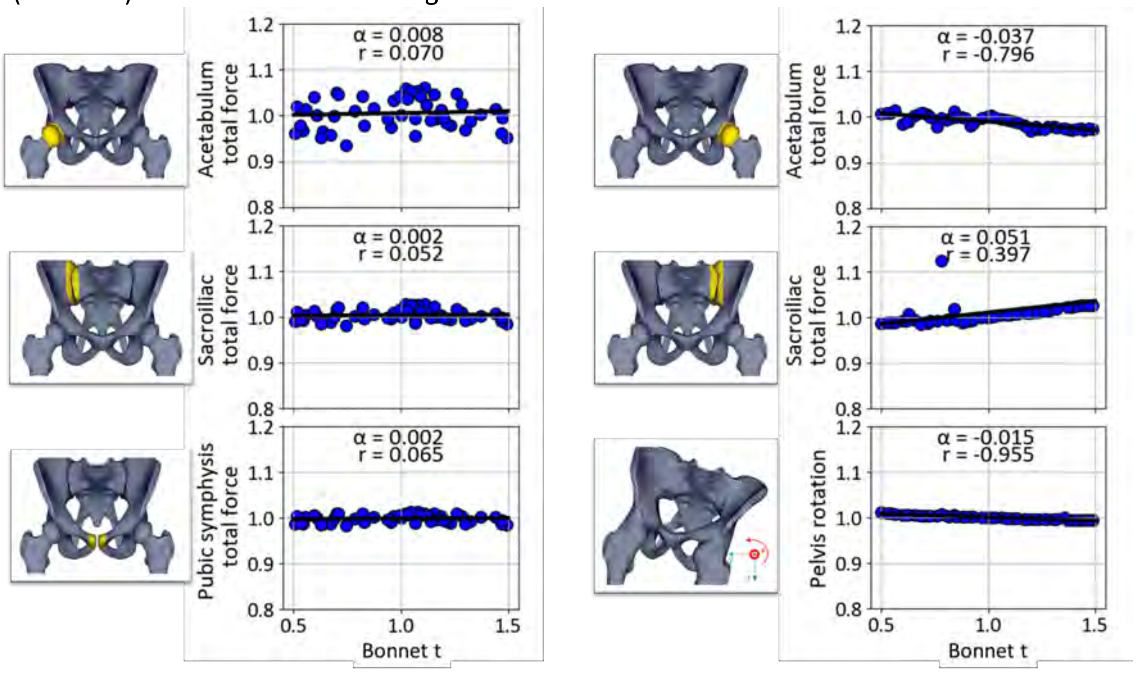

(a) non-struck side (b) struck side

Fig. 6. Normalised maximum pelvis measurements at test position Y0 for the SUV by varying the exterior sheet thickness of the bonnet.

A stiffer bonnet in the vertical direction shows a decreased left acetabulum joint total force (struck side) and an increased left sacroiliac joint total force (struck side) with decent correlation and meaningful slopes ($r > |0.39|$ and $\alpha > |0.03|$). The non-struck side acetabulum and sacroiliac joint total forces as well as the pubic symphysis total force are unaffected ($r < 0.07$ and $\alpha < 0.01$). The pelvis rotation around the sagittal axis (x-axis in Figure 6) decreases as the bonnet thickness increases.

Variation of Vertical Stiffness at Test Position Y+600

The aPLI, HBM and child headform impactor results for the vertically stiffer BLE (variation of the bonnet's exterior sheet thickness) for the SUV at test position Y+600 are shown in Figure 7 and Figure 8. Figure 7 contains the results for the leg and head measurements and Figure 8 contains the HBM pelvis measurements.

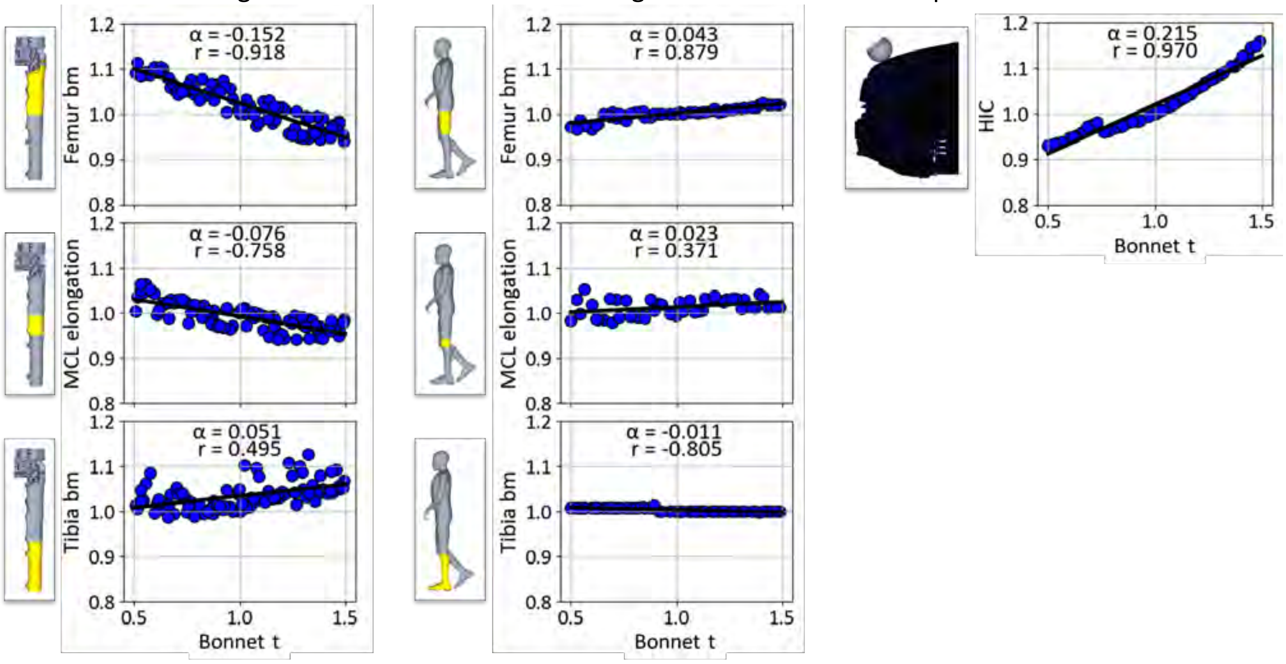

(a) aPLI (b) HBM (c) Child headform impactor

Fig. 7. Normalised maximum injury values for (a) the aPLI, (b) the HBM leg and (c) the child headform impactor (HIC) at test position Y+600 for the SUV by varying the exterior sheet thickness of the bonnet.

A stiffer bonnet in the vertical direction shows a considerably decreased femur bending moment and MCL elongation for the aPLI ($r > |0.75|$ and $\alpha > |0.07|$). However, the results also indicate contrary tendencies for the HBM's femur bending moment and MCL elongation. In addition, a thicker bonnet leads to an increase in both the aPLI's maximum tibia bending moment and the HIC for the child headform impactor.

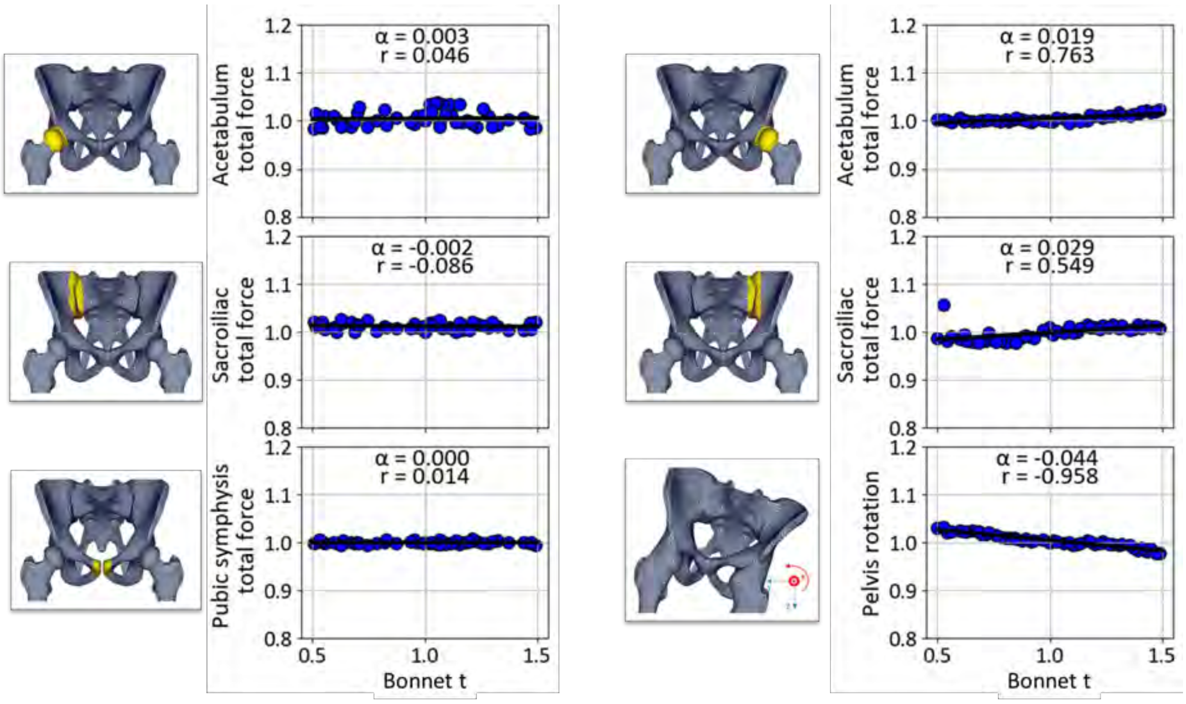

(a) non-struck side (b) struck side

Fig. 8. Normalised maximum pelvis measurements at test position Y+600 for the SUV by varying the exterior sheet thickness of the bonnet.

A stiffer bonnet in the vertical direction increases the total forces for the struck-side (r > 0.5 and α > 0.019). The non-struck side and pubic symphysis values, however, are unaffected. Again, the pelvis rotation decreases as the bonnet thickness increases.

Variation of Horizontal Stiffness

Figure 9 illustrates the influence of added ribs in the front part of the BLE between the exterior and interior sheet for both test positions.

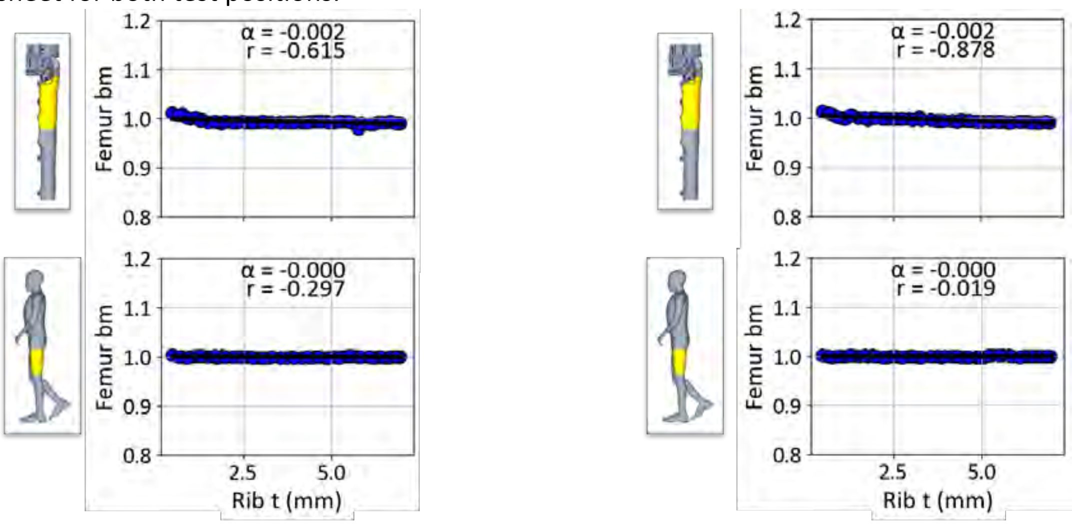

(a) Y0 (b) Y+600

Fig. 9. Normalised maximum femur bending moments for the aPLI and HBM at test position (a) Y0 and (b) Y+600 by varying the rib thickness between exterior and interior sheet.

The added ribs show negligible effects on the injury values. A stiffer BLE in horizontal direction is therefore not investigated further. However, the results of a horizontally weaker BLE due to the modification of the support part are shown in Figure 10.

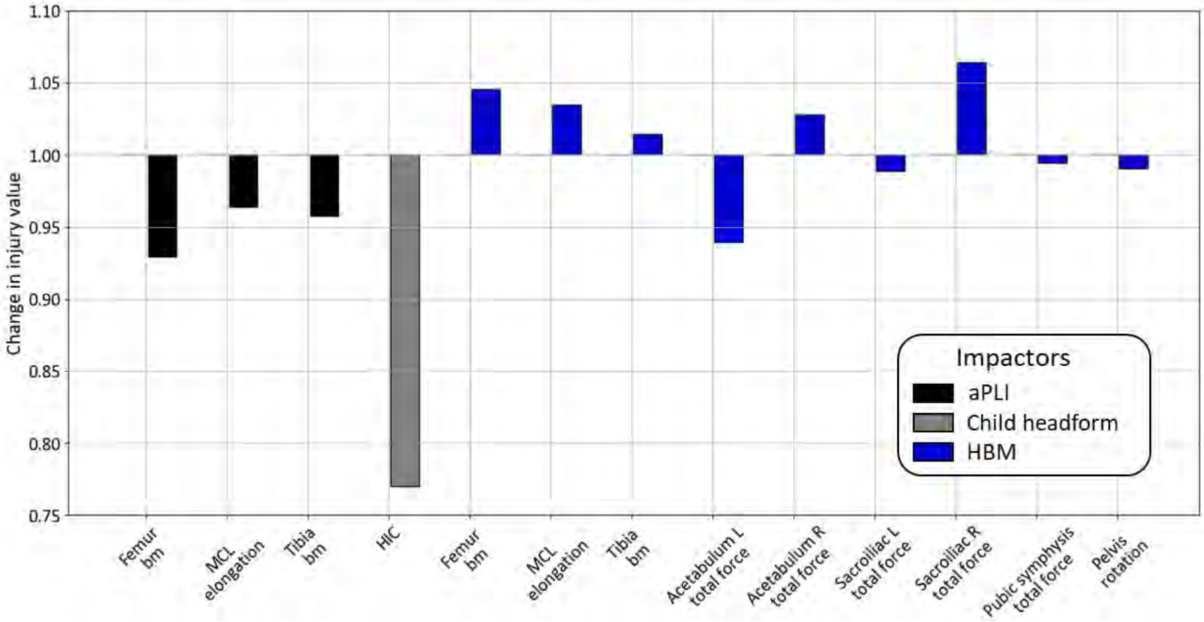

(a) Change in injury value due to the modification at test position Y0

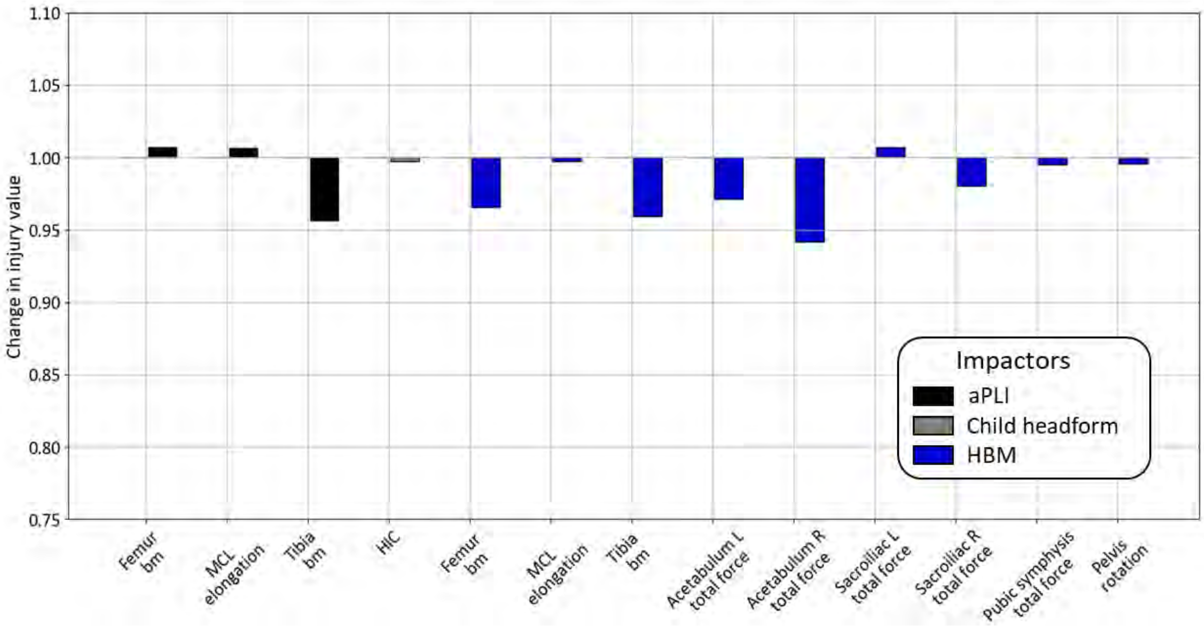

(b) Change in injury value due to the modification at test position Y+600

Fig. 10. Change in maximum injury value due to the modification of the support part in relation to the original support part for test position Y0 (a) and test position Y+600 (b).

The changes in the injury values in the Figures 10a and 10b due to the modified support part (Figure 3b) are based on the injury values with the original support part shown in Figure 3a (normalised to 1.0). The reduced horizontal stiffness of the BLE due to the modified support part leads to a significantly reduced HIC value (-23% compared to the original value) and reduced aPLI injury values (-7% femur bm, -4% MCL elongation and -4% tibia bm compared to the original values) at test position Y0. However, simultaneously, the femur, MCL and tibia values increase for the HBM (+5% femur bm, +3% MCL elongation and +1% tibia bm). Due to the modification, a horizontal intrusion of the femur is possible for both the HBM and aPLI. The intrusion is greater for the HBM femur due to its higher weight, resulting in increased injury values. While a *slight intrusion*, as seen in the aPLI, may be beneficial, a larger intrusion, as seen in the HBM (approximately double the aPLI intrusion), is counterproductive.

At test position Y+600 the aPLI tibia bm decreases by 4% and the remaining aPLI measurements are rather unaffected (change < 1%), while the HBM femur bm, MCL elongation and tibia bm decrease (-3% femur bm, -1% MCL elongation and -4% tibia bm). The leg results are corresponding to the Y0 observation of benefiting from a *slight intrusion*. Overall, the intrusion at Y+600 is lower compared to Y0 due to greater outwards rotation and movement of both the HBM and aPLI. This leads to the desired *slight intrusion* for the HBM and a negligible intrusion for the aPLI in horizontal direction.

The pelvis measurements decrease for the struck-side (abbreviated L in Figure 10) and increase for the non-struck side (abbreviated R in Figure 10) at test position Y0 and show mixed results at test position Y+600. For the pelvis values (Acetabulum, Sacroiliac and Pubic symphysis), the Acetabulum total force L (struck side) is the highest measured force by far (about 5 times higher than the sacroiliac and pubic symphysis total forces) at both test positions, too. Therefore, as the modification reduces the aPLI, HIC and HBM Acetabulum total forces L (struck side), we consider the modification successful and use it as baseline to investigate a vertical stiffness and shooting height variation. Nonetheless, we want to emphasise that designing this *slight intrusion* is very front-end package dependent and has to be done carefully.

Variation of Vertical Stiffness and Shooting Height for the Softer Horizontal Bonnet Leading Edge at Test Position Y0

Figure 11 contains the relevant contour plots at test position Y0 for both the aPLI and the HBM. The complete set of contour plots for test position Y0 displaying all the aPLI and HBM injury criteria can be found in the Appendix (Figure A1-A4).

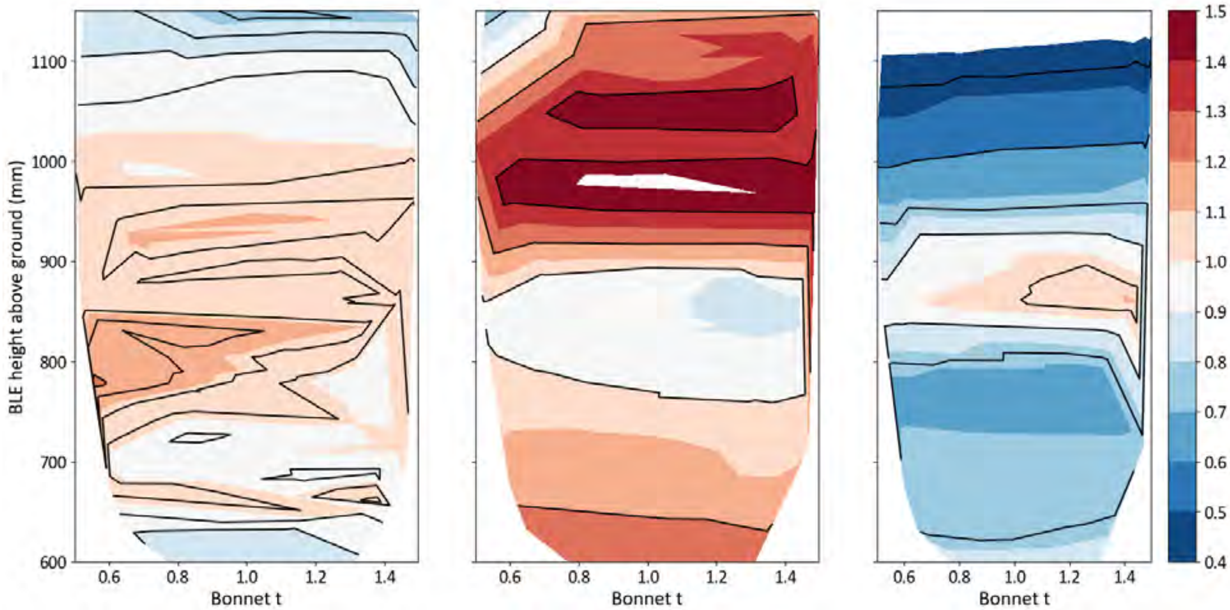

(a) aPLI femur bm (b) HBM femur bm (c) Acetabulum L total force

Fig. 11. Normalised maximum injury values at test position Y0 for the SUV by varying the exterior sheet thickness of the bonnet and the shooting height of the impactor (converted to BLE height above ground).

The aPLI femur bending moment (Figure 11a) peaks at 780 mm BLE height and the HBM femur bending moment (Figure 11b) peaks at 1050 mm BLE height. The HBM femur bending moment shows an opposite trend to the aPLI femur bending moment as it increases gradually below 800 mm BLE height and above 900 mm BLE height whereas the aPLI femur bending moment decreases gradually below 800 mm BLE height and above 900 mm BLE height. A thicker bonnet's exterior sheet seems to reduce the aPLI femur bending moment at its peak's BLE height of 780 mm. For the HBM femur bending, a thicker bonnet's exterior sheet seems to reduce the HBM femur bending at its peak's BLE height of 1050 mm.

The acetabulum total force, measured at the struck leg, peaks at a BLE height of 850 mm and decreases for smaller and taller vehicles. A thicker bonnet's exterior sheet seems to increase the force at its peak's BLE height of 850 mm. For all other BLE heights, the influence of the bonnet's exterior sheet thickness seems negligible.

Variation of Vertical Stiffness and Shooting Height for the Softer Horizontal Bonnet Leading Edge at Test Position Y+600

Figure 12 contains the relevant contour plots at test position Y+600 for both the aPLI and the HBM. Again, the complete set of contour plots for test position Y+600 displaying all the aPLI and HBM injury criteria can be found in the Appendix (Figure A5-A8).

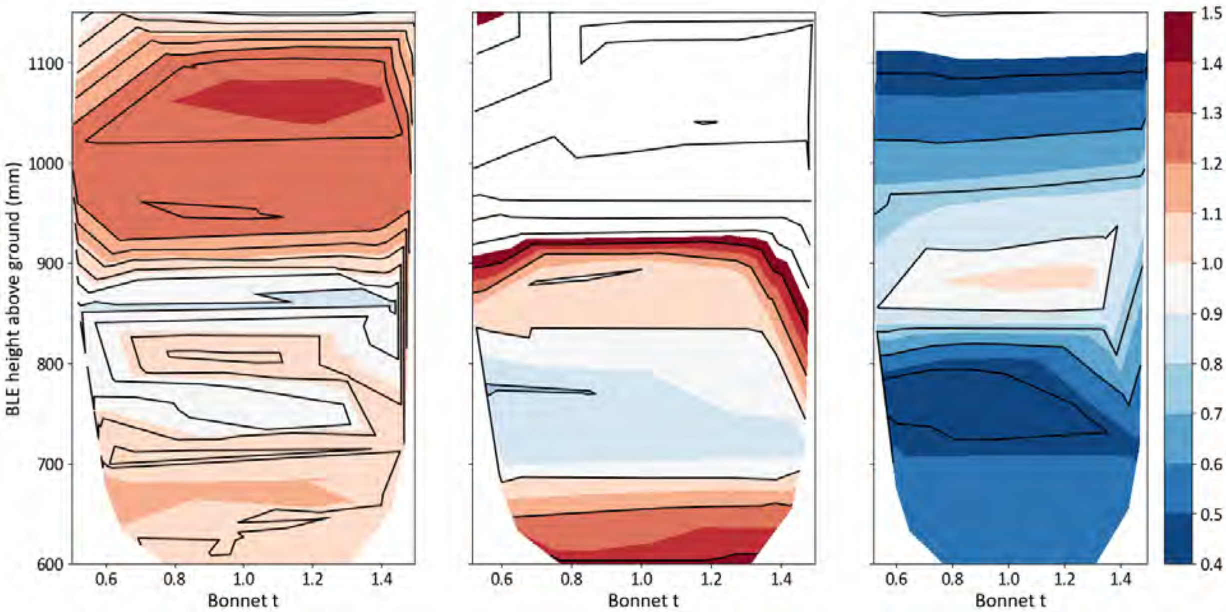

(a) aPLI femur bm (b) HBM femur bm (c) Acetabulum L total force

Fig. 12. Normalised maximum injury values at test position Y+600 for the SUV by varying the exterior sheet thickness of the bonnet and the shooting height of the impactor (converted to BLE height above ground).

The aPLI femur bending moment (Figure 12a) peaks at 1050 mm BLE height and at 650 mm BLE height. The HBM femur bending moment (Figure 12b) peaks at 900 mm BLE height and at 600 mm BLE height. A thicker bonnet's exterior sheet seems to reduce the aPLI femur bending moment at its peaks' BLE heights. For the HBM femur bending, the bonnet thickness seems negligible.

The acetabulum total force, measured at the struck leg, peaks at a BLE height of 880 mm and decreases for smaller and taller vehicles. A thicker bonnet's exterior sheet seems to decrease the force at its peak's BLE height of 880 mm. For all other BLE heights, the influence of the bonnet's exterior sheet thickness seems negligible.

IV. Discussion

Reducing lower extremity injury risk while considering pelvis and head injury risk is a necessary task in road safety for increasing vehicle front-end heights. However, the relationships between the vehicle front-end parameters and the various injury measurements are quite unknown. Therefore, this study examines the BLE of a single SUV for the aPLI injury criteria, pelvis contact forces with the HBM and HIC with the child headform impactor.

The variation of the BLE's vertical stiffness (variation of exterior sheet thickness) shows that the aPLI femur bending moment and MCL elongation at both test positions (Y0 and Y+600) decrease with a vertically stiffer bonnet (single digit percentages). The HBM confirms this trend at test position Y0. At test position Y+600, however, the aPLI's SUBP absorbs more strain energy compared to the pelvis of the HBM. Figure 13 shows this larger deformation of the BLE. By increasing the vertical stiffness, the intrusion of the SUBP is reduced which subsequently reduces the bending within the leg part of the aPLI. This trend at test position Y+600 (significantly decreasing the aPLI injury values with a vertically stiffer BLE), shown in Figure 7, is the result of an inflated, non-biofidelic rotation of the SUBP, which absorbs more strain energy than the HBM's pelvis.

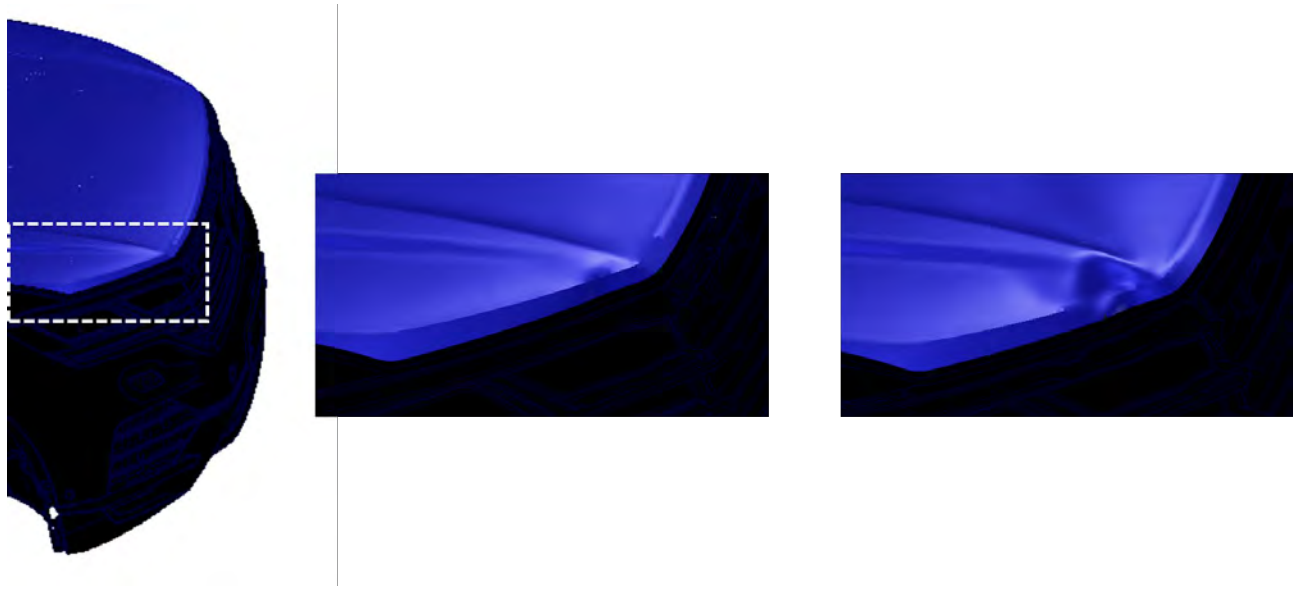

(a) Pre-Crash bonnet (b) HBM impact at t = 25 ms (c) aPLI impact at t = 25 ms

Fig. 13. Pre-Crash configuration of the bonnet with highlighted impact area (a). Deformation state of the bonnet leading edge at test position Y+600 for the HBM impact (b) and for the aPLI impact (c).

The acetabulum joint total force at the struck side (left pelvis of the HBM) is the by far highest measured pelvis joint force across all simulations (about 5 times higher than the sacroiliac joint total force at struck side or the pubic symphysis total force). It decreases significantly for a vertically stiffer BLE at Y0 and is slightly increased for a vertically stiffer BLE at Y+600. The HIC, however, shows a clear trend that the lower the vertical stiffness, the better the result.

The variation of the BLE's horizontal stiffness shows that the original configuration is stiff. The modification of the support part (Figure 3) leads to a weaker horizontal stiffness and shows that the HIC at test position Y0 decreases significantly. Additionally, the acetabulum joint total forces at the struck side (left pelvis of the HBM) decrease for both test positions, while the aPLI injury values decrease especially for test position Y0. Overall, the variation in horizontal stiffness of the BLE indicates that a lower horizontal stiffness is preferable for pedestrian safety. However, excessively low stiffness may have a negative impact.

The variation of vertical stiffness and shooting height based on the modified support part (reduced horizontal stiffness compared to the original vehicle) shows that vehicle height influences the injury values significantly (50% reduced injury values possible). At critical vehicle heights, an adequate vertical stiffness can achieve reductions of around 10%.

For test position Y0, the aPLI femur bending moment and the HBM acetabulum total force at the struck leg decrease for taller and smaller vehicles (BLE height > 900 mm and BLE height < 750 mm). The HBM femur bending moment, however, increases for taller and smaller vehicles. This contrast in femur bending may be due to the difference between aPLI SUBP and HBM upper body. For tall vehicles, the aPLI gets pushed directly towards the ground without inducing bending moments whereas the HBM still bends over the vehicle due to its height and induces bending moments. For small vehicles, the HBM exhibits more horizontal deformation in the BLE area than the aPLI due to its higher weight. This increased deformation leads to higher femur bending in the HBM. An increased bonnet's exterior sheet thickness is desirable for critical aPLI and HBM femur bending BLE heights. For critical acetabulum total force BLE heights, however, a thicker exterior sheet is not desirable.

For test position Y+600, the aPLI femur bending moment peaks at 1050 mm BLE height and at 650 mm BLE height. The HBM femur bending moment peaks at 900 mm BLE height and at 600 mm BLE height. A thicker bonnet's exterior sheet reduces the aPLI femur bending moment at its peaks' BLE heights but does not affect the HBM femur bending moment at its peaks' BLE heights. The HBM acetabulum total force, measured at the struck leg, peaks at 880 mm and decreases with a thicker bonnet's exterior sheet. Overall, the investigation at test position Y+600 indicates that a thicker bonnet's exterior sheet decreases the injury values for critical BLE heights.

Summarising the findings of this study, smaller vehicle front-ends can help to reduce the injury values. However, it should be noted that lower vehicle fronts usually have completely different packages and geometries, resulting in different pedestrian kinematics and pedestrian-component contacts. Therefore, the transferability of the reported potential of about 50% lower injury values is limited. A horizontally deformable BLE is beneficial for pedestrian protection (too deformable seems to be counterproductive though). Starting with a horizontally deformable BLE, a vertically stiffer BLE (compared to the original, state of the art vehicle) helps to decrease the most important leg and pelvis injury values at test position Y+600 for critical BLE heights (at the right headlight from driver's perspective). To address the subsequently increasing HIC values for a vertically stiffer BLE, future work could explore a load case dependent vertical stiffness configuration of the BLE (very weak for head impact and stiffer for leg/pelvis impact). However, these statements are solely based on one gait position of a 50th percentile male surrogate, which limits applicability for generalisation. Additionally, the variation of shooting height, which we converted to BLE height above ground level does not perfectly represent different vehicles with different BLE heights, but rather approximates different pedestrian heights. Furthermore, the normalised representation of the injury values with respect to the original vehicle limits the transferability. Nonetheless, we demonstrate that the widely accepted practice of designing soft vehicle front-ends for pedestrian safety may not be applicable to the BLEs of SUVs in vertical direction and requires careful analysis.

V. Conclusions

This study highlights that design decisions for the optimisation of one body region or injury criterion can compromise other body regions and injury criteria. Consequently, we would like to make a recommendation for future studies to consider different injury criteria for vehicle front-end components that appear to affect body regions in different ways. This would help to avoid the potential for conflicts of interest to be overlooked. A horizontally weaker BLE compared to the state of the art SUV helps to decrease the leg, pelvis and head injury values for both test positions Y0 and Y+600. A thicker bonnet's exterior sheet helps to decrease the leg and pelvis values for test position Y+600 but increases the HIC value, which gives rise of motivation to actively control the BLE's vertical stiffness depending on the individual load case. For test position Y0, a weaker BLE is desired. However, by exclusively using the 50th percentile male HBM, the transferability of the results is limited, which we tried to address by the variation of shooting height. For future research, enhancing the transferability of the study could be achieved by extending it to include different vehicle front packages, various vehicle types (such as minivans and pickup trucks) and incorporating the 5th percentile female HBM.

VI. References

[1] World Health Organization. Global Status Report on Road Safety 2018. Technical report, 2018.

[2] National Highway Traffic Safety Agency. Traffic Safety Facts 2021. Technical report, 2023.

[3] Network. Global Burden of Disease Study 2019. *Institute for Health Metrics and Evaluation* (IHME): Seattle, Washington, USA, 2019.

[4] Otte, D., Jänsch, M., Haasper, C. Injury protection and accident causation parameters for vulnerable road users based on German In-Depth Accident Study GIDAS. *Accident Analysis and Prevention*, 2012, 44(1):149-53.

[5] Harden, A., Kan, Y-S., Baker, G., Stull, K., Agnew, A. Exploring the effects of sex and size on dynamic tibia properties. *Proceedings of IRCOBI Conference*, 2023, Cambridge, England.

[6] Mizuno, Y. Summary of IHRA Pedestrian Safety WG Activities (2005)-Proposed test methods to evaluate pedestrian protection afforded by passenger cars. *Proceedings of International Technical Conference on the Enhanced Safety of Vehicles*, 2005, Washington D.C., USA.

[7] Li, G., Otte, D., Yang, J., Simms, C. Pedestrian Injury Trends Evaluated by Comparison of the PCDS and GIDAS Databases. *Proceedings of IRCOBI Conference*, 2016, Seoul, South Korea.

[8] Gómez Vilches, J., Pasqualino, R., Hernandez Y. The new electric SUV market under battery supply constraints: Might they increase CO2 emissions*? Journal of Cleaner Production*, 2023, 383, 135294.

[9] International Energy Agency (IEA), Share of SUVs in total car sales in key markets, 2010-2019. Report, 2020, Paris, France.

[10] Chiapedi, S. Flexibility-Oriented Design Guidelines for Pedestrian Leg Impact on the Basis of a Low-Fidelity Vehicle Front-End Model, PhD Thesis. Germany: Technical University of Munich, 2021.

[11] Mößner, S. Multi-fidelity Structural Design for Pedestrian Safety with particular Reference to the FlexPLI. PhD Thesis. Germany: Technical University of Munich, 2019.

[12] Chiapedi, S., Koukal, A., Duddeck, F. Sensitivity Analysis for Pedestrian Lower Leg Impact. *Proceedings of the 7th GACM Colloquium on Computational Mechanics for Young Scientists from Academia and Industry*, 2017 Stuttgart, Germany.

[13] Klug, C., Weinberger, M., et al. Pelvic and femoral injuries in car-to-pedestrian accidents. *Proceedings of IRCOBI Conference*, 2015, Lyon, France.

[14] Isemann, D., Lehmann, K., Böhme, M., Kröger, M. Effects of Impact Side on Medial Collateral Ligament Elongation during Vehicle–Pedestrian Impact. *Proceedings of IRCOBI Conference*, 2023, Cambridge, England.

[15] Isshiki, T., Antona-Makoshi, J., Konosu, A., Takahashi, Y. Consolidated Technical Specifications for the Advanced Pedestrian Legform Impactor (aPLI). *Proceedings of IRCOBI Conference*, 2018, Athens, Greece.

[16] Teichmann, C., A comparison between aPLI and HBM simulation. *Carhs Praxis Conference Pedestrian*, 2020, Bergisch Gladbach, Germany.

[17] Jani, D., Lehmann, K., Teichmann, C., Marini, G. Effect of the Lower Limb Muscles on the Knee Lateral Bending and Medial Collateral Ligament's Elongation during Vehicle – Pedestrian Impacts. *Proceedings of IRCOBI Conference*, 2021.

[18] Staack, H., Teichmann, C., Lehmann, K. Influence of Pedestrian Impact Direction to MCL Elongation. *Carhs Praxis Conference Pedestrian*, 2021, Bergisch Gladbach, Germany.

[19] Untaroiu, C., Meissner, M., Crandall, J., Takahashi, Y., Okamoto, M., Ito, O. Crash reconstruction of pedestrian accidents using optimization techniques. *International Journal of Impact Engineering*, 2009, 36(2):210-219.

VII. APPENDIX

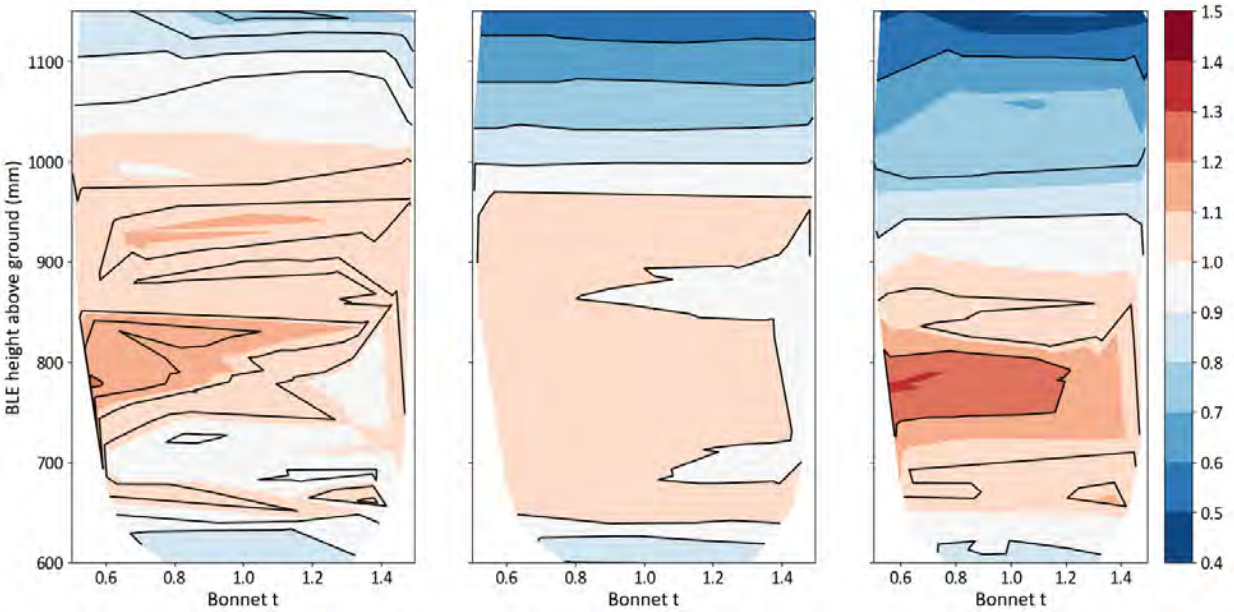

(a) Femur bm (b) MCL elongation (c) Tibia bm

Fig. A1. Normalised maximum aPLI injury values at test position Y0 for the SUV by varying the exterior sheet thickness of the bonnet and the shooting height of the impactor (converted to BLE height above ground).

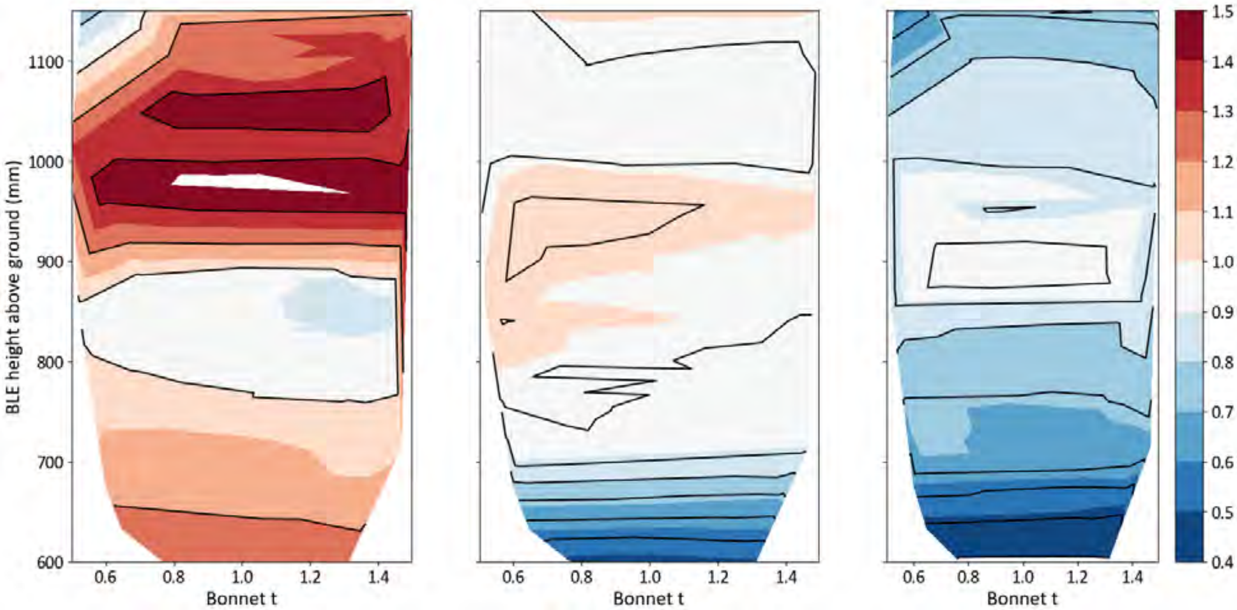

(a) Femur bm (b) MCL elongation (c) Tibia bm

Fig. A2. Normalised maximum HBM leg injury values at test position Y0 for the SUV by varying the exterior sheet thickness of the bonnet and the shooting height of the HBM (converted to BLE height above ground).

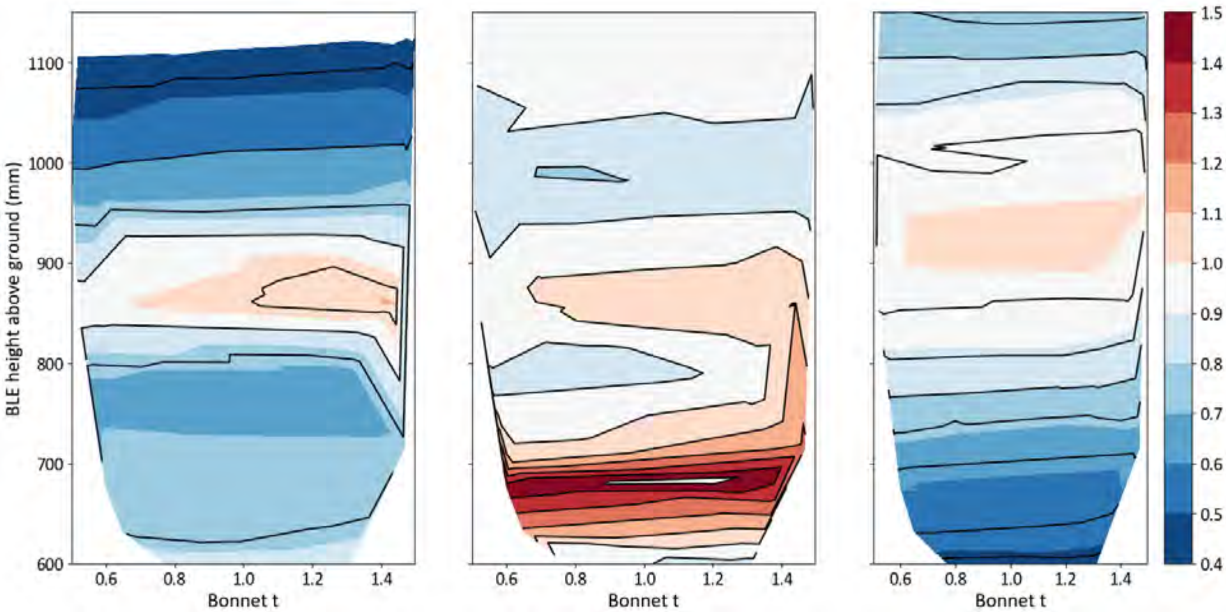

(a) Acetabulum L total force (b) Sacroiliac L total force (c) Pelvis rotation

Fig. A3. Normalised maximum HBM pelvis injury values for the struck side (left pelvis of the HBM) at test position Y0 for the SUV by varying the exterior sheet thickness of the bonnet and the shooting height of the HBM (converted to BLE height above ground).

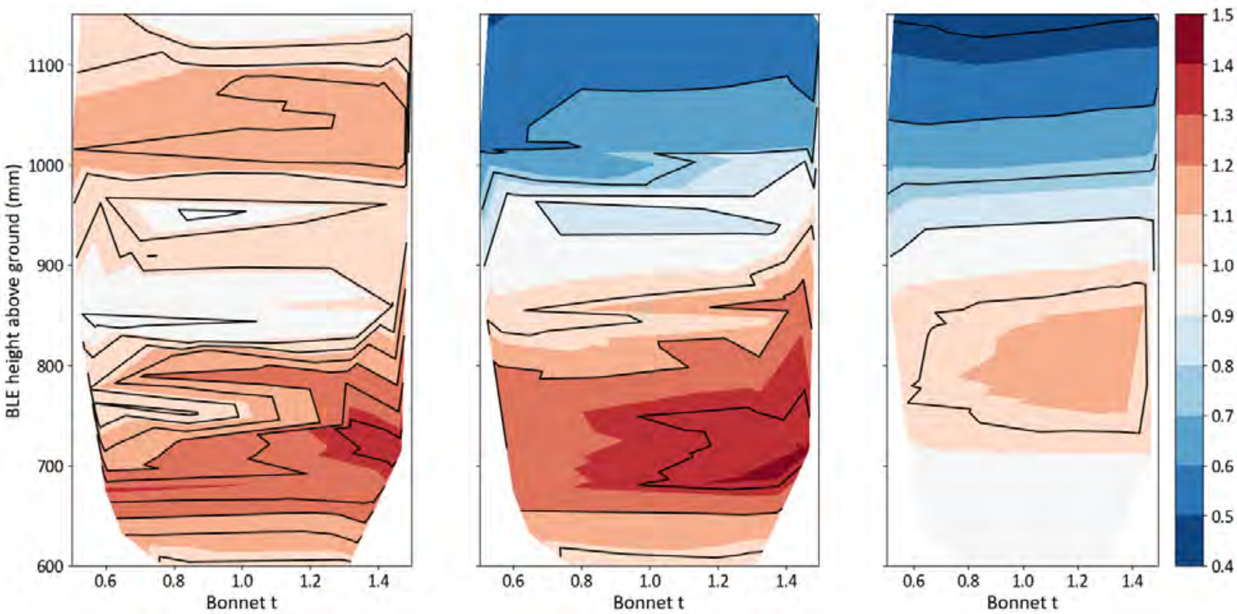

(a) Acetabulum R total force (b) Sacroiliac R total force (c) Pubic symphysis total force

Fig. A4. Normalised maximum HBM pelvis injury values for the non-struck side (right pelvis of the HBM) at test position Y0 for the SUV by varying the exterior sheet thickness of the bonnet and the shooting height of the HBM (converted to BLE height above ground).

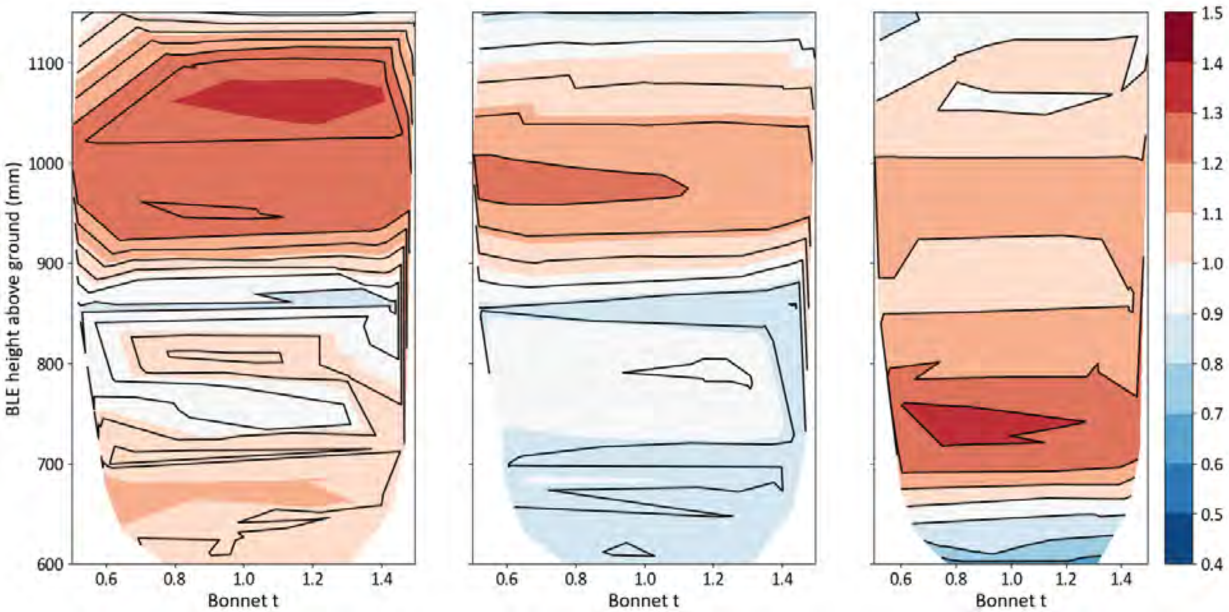

(a) Femur bm (b) MCL elongation (c) Tibia bm

Fig. A5. Normalised maximum aPLI injury values at test position Y+600 for the SUV by varying the exterior sheet thickness of the bonnet and the shooting height of the impactor (converted to BLE height above ground).

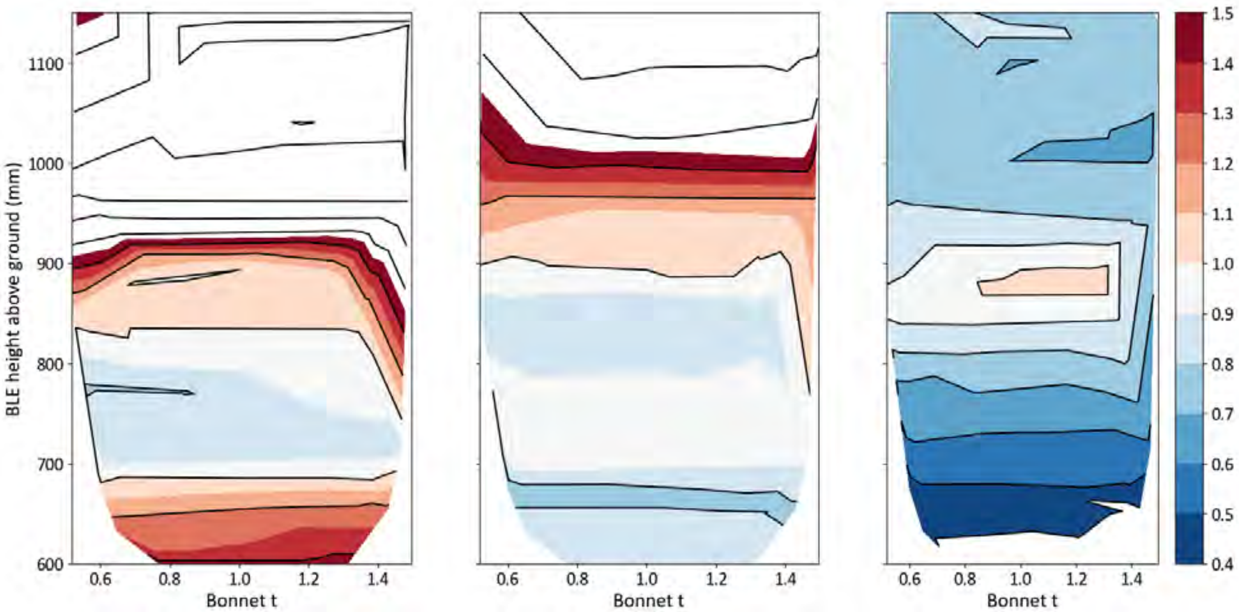

(a) Femur bm (b) MCL elongation (c) Tibia bm

Fig. A6. Normalised maximum HBM leg injury values at test position Y+600 for the SUV by varying the exterior sheet thickness of the bonnet and the shooting height of the HBM (converted to BLE height above ground).

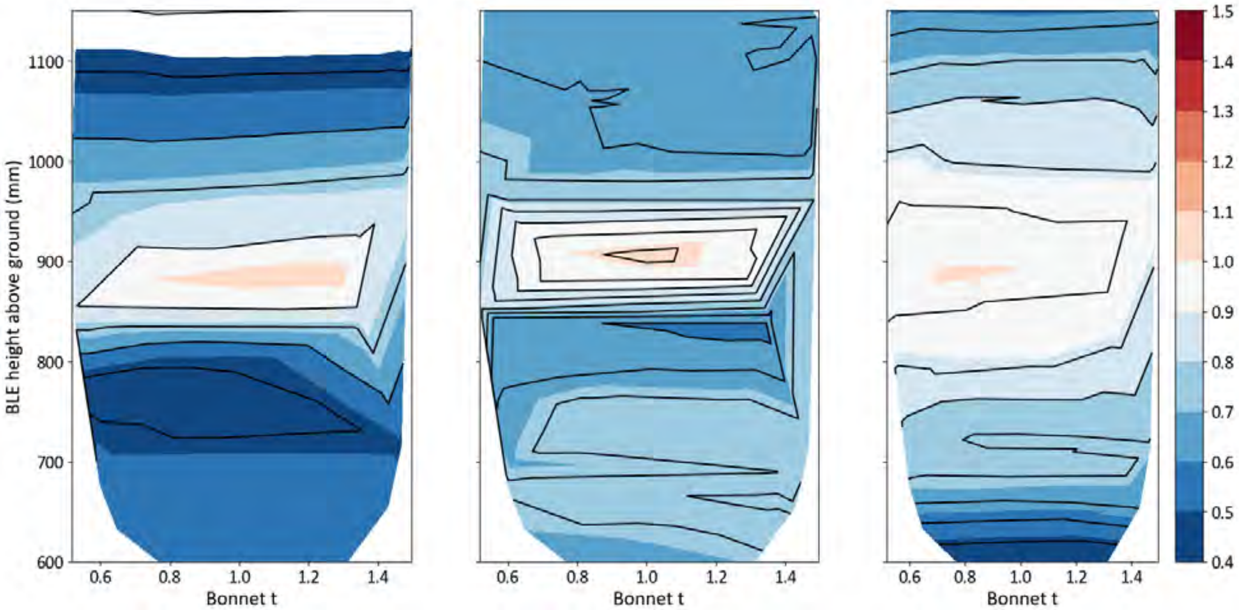

(a) Acetabulum L total force (b) Sacroiliac L total force (c) Pelvis rotation

Fig. A7. Normalised maximum HBM pelvis injury values for the struck side (left pelvis of the HBM) at test position Y+600 for the SUV by varying the exterior sheet thickness of the bonnet and the shooting height of the HBM (converted to BLE height above ground).

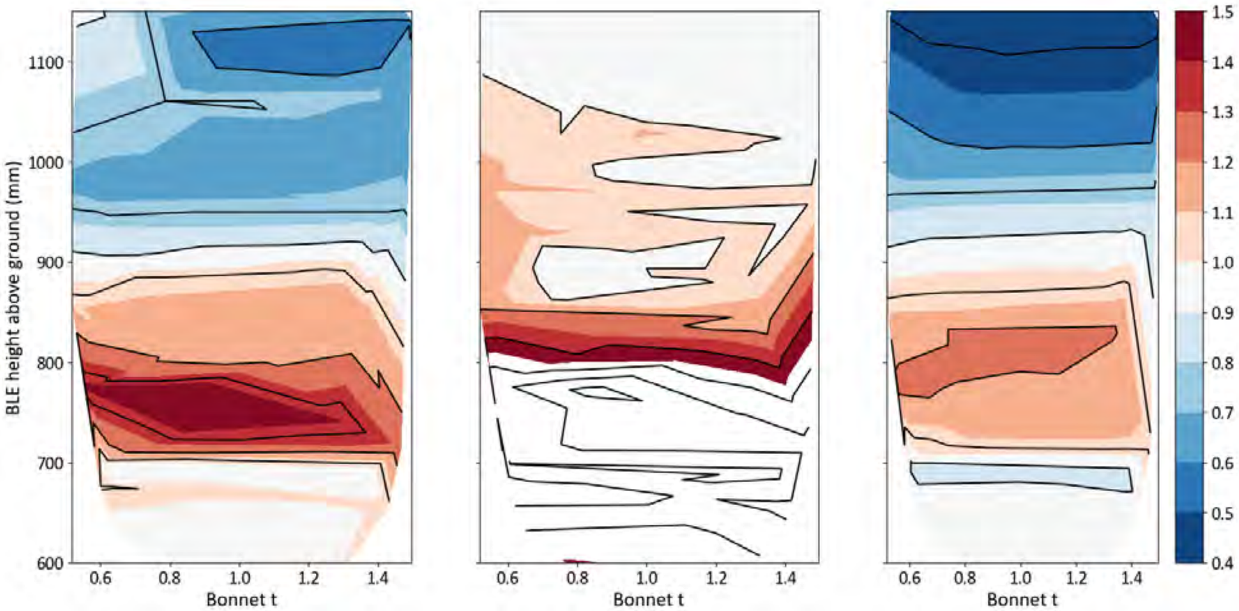

(a) Acetabulum R total force (b) Sacroiliac R total force (c) Pubic symphysis total force

Fig. A8. Normalised maximum HBM pelvis injury values for the non-struck side (right pelvis of the HBM) at test position Y+600 for the SUV by varying the exterior sheet thickness of the bonnet and the shooting height of the HBM (converted to BLE height above ground).